



# Groundwater quality index as a hydrochemical tool for monitoring saltwater intrusion into coastal freshwater aquifer of Eastern Dahomey Basin, Southwestern Nigeria

Jamiu A. Aladejana<sup>a,b,\*</sup>, Robert M. Kalin<sup>a</sup>, Philippe Sentenac<sup>a</sup>, Ibrahim Hassan<sup>a,c</sup>

<sup>a</sup> Department of Civil and Environmental Engineering University of Strathclyde Glasgow, UK

<sup>b</sup> Department of Geology, University of Ibadan, Nigeria

<sup>c</sup> Department of Civil Engineering Abubakar Tafawa Balewa University Bauchi, Nigeria

## ARTICLE INFO

### Keywords:

Saltwater intrusion

Groundwater quality index

Freshwater and Coastal aquifer

## ABSTRACT

Saltwater intrusion into coastal freshwater aquifers is a threat to groundwater quality globally. This study aims to determine the extent of saltwater intrusion into the coastal freshwater aquifer of the Eastern Dahomey Basin (EDB), Nigeria. Groundwater chemistry was sampled and analysed for ionic ratios and interpreted using a hydrochemical facie evolution diagram (HFE-D), the saltwater mixing index (SMI) and the Groundwater quality index for saltwater intrusion (GQIswi). High EC and TDS and the concentration of dissolved ions showed increased salinity as a result of seawater intrusion in wells located around communities in Seme, Lekki, Eleko, Okun-Ajah, Ode-Mahin and Igbokoda. Correlation of ions in the wet season also suggests higher salinities which originate partly from industrial and municipal effluents especially from wells which are close to river channels, while dry season groundwater shows the dominant influence of seawater intrusion. HFE-D revealed that mixed groundwater of Na + Ca-HCO<sub>3</sub>, Na-Cl and Ca-Cl dominate the area due to gravity-driven flow leading to groundwater freshening inland from the coastline towards the northern part of the basin. The groundwater quality index from SMI and GQIswi shows areas within 3 km from the coastline that are more sensitive to saltwater intrusion based on abstraction rate and depth of the wells. The present study provides information of value to planners and policy-makers for the sustainable management and protection of coastal groundwater resources in the Eastern Dahomey Basin.

## 1. Introduction

Coastal aquifers around the world are at risk of increasing salinity resulting from saltwater intrusion. Rapid growth in urbanisation, population and the associated over-abstraction of groundwater in coastal regions has worsened the situation. Mapping the intrusion and extent of saltwater coverage or mixing zones is difficult and costly due to the hydrogeologic complexity, the multifaceted nature of the problem, and the high cost of drilling multiple level wells needed for detailed study (Custodio, 2005).

Nigeria, the most populous nation in Africa, has some of its largest cities on the southwestern coast (Ukhurebor and Abiodun, 2018). The high population density has resulted in over-abstraction of groundwater from the fragile coastal aquifer, and the proximity to the sea has led to a saltwater intrusion into the coastal freshwater aquifer. Studies have

shown that saline groundwater can lead to severe problems for water supply, especially under heavy groundwater abstraction (Tirkey et al., 2017). Seawater intrusion is a widespread problem of coastal aquifers associated with urbanisation (Han et al. (2016), Oteri and Atolagbe (2003), Longe et al.; (1987), Adepelumi et al.; (2009), Adeoti et al.; (2010), Ayolabi et al.; (2013) and Talabi et al. (2012)). These studies identified saline water in some boreholes and wells especially at the upper-aquifer in part of Lagos. Some of the locations experiencing saline water intrusion include the eastern coast of Lagos such as Lekki, Ajah, Victoria Island and coastal communities in Ondo state such as Aiyetoro, Ugbonla, Mahin and Igbokoda. The origin of saltwater was linked to the incursion of seawater from the ocean during the flooding of canals and dissolved evaporites trapped within the aquifers sediments. Adelana et al. (1996) observed that deterioration of water quality in the coastal zones of Lekki phase 1 and Oniru environs of Lagos metropolis is due to

\* Corresponding author. Department of Civil and Environmental Engineering University of Strathclyde Glasgow, UK.

E-mail address: [Jamiu.aladejana@strath.ac.uk](mailto:Jamiu.aladejana@strath.ac.uk) (J.A. Aladejana).

<https://doi.org/10.1016/j.gsd.2021.100568>

Received 6 January 2020; Received in revised form 30 October 2020; Accepted 24 February 2021

Available online 13 March 2021

2352-801X/Crown Copyright © 2021 Published by Elsevier B.V. This is an open access article under the CC BY-NC-ND license

(<http://creativecommons.org/licenses/by-nc-nd/4.0/>).

saltwater intrusion which was of concern among the owner of properties in the vicinity. They also found several boreholes constructed in Naira were abandoned due to saline water intrusion.

Cities underlying by the Eastern Dahomey Basin, like other coastal cities in the world, rely heavily on the groundwater resources as one source of potable water for domestic, industrial and agricultural purposes to complement the erratic pipe-borne water supply. There are a few specific-sites hydrogeological studies of the area within the basin especially approaching the border with Lagos (Longe et al., 1987; Oteri and Atolagbe, 2003; Longe and Balogun, 2010) while few or none have looked at hydrogeological processes across the entire basin to study the relative distribution and extent of saline intrusion and its effect on groundwater quality. These aquifers constitute a vital source of freshwater in the regions, and with the continuous increase in water demand there is vital need to monitor the risk of saline water intrusion as once this problem occurs it is difficult to remediate. A long-term water resource management strategy is needed which will require investment. Less than 2% of seawater intrusion in the freshwater can diminish the water's potability according to Custodio, 2005. Presently, there is no groundwater monitoring well within this basin, necessary for routine saltwater intrusion monitoring. Assessment of major ions is vital to identify the source of determination of water quality (Saha et al., 2018). The chemical composition of groundwater changes as it flows through geologic media, so full chemical analysis is useful to identify a saltwater intrusion (Saha et al., 2019; Seddiqie et al., 2019).

This study employed hydrochemical methods using selected

groundwater indices and ionic ratios to fingerprint saline water intrusion in freshwater. The conclusions are expected to be considered as one monitoring tool for the annual assessment of groundwater in the coastal aquifers of the EDB. The indices used include hydrochemical evolution facies diagram HEF diagram, Groundwater Quality Index for Saltwater Intrusion (GQIswi) and Seawater Mixing Index (SMI), combined with the ionic ratios Br/Cl and Cl/HCO<sub>3</sub> and Revelle coefficient. These methods had proven effective in the work of Kennedy (2012), Christina and Alexandros (2014); Amiri et al. (2016) and Edet (2016). Comparing these indices and ratios should support policy for groundwater monitoring for saltwater intrusion. The outcomes will add to available information and knowledge on the saltwater intrusion of the coastal freshwater aquifer of the EDB. This information is necessary for sustainable groundwater resources management in this coastal zone in the face of both anthropogenic and natural drivers, such as climate change.

1.1. Study area and geomorphology

The Eastern Dahomey Basin lies in the southwestern part of Nigeria (Fig. 1). It is a transboundary basin that extends from Ghana through Togo and Benin to Nigeria. This basin is bounded by Okitipupa Ridge, which is the boundary it shares with Niger Delta basin (Jones and Hockey, 1964). It lies between Latitudes 2°41'10.00" - 4°59'5900"N and Longitudes 6°21'1300" - 7°52'42.00"E along the coast of the Gulf of Guinea. The basin is bounded in the south by the Atlantic Ocean, and thin out at the north by the Precambrian basement rocks. The area of

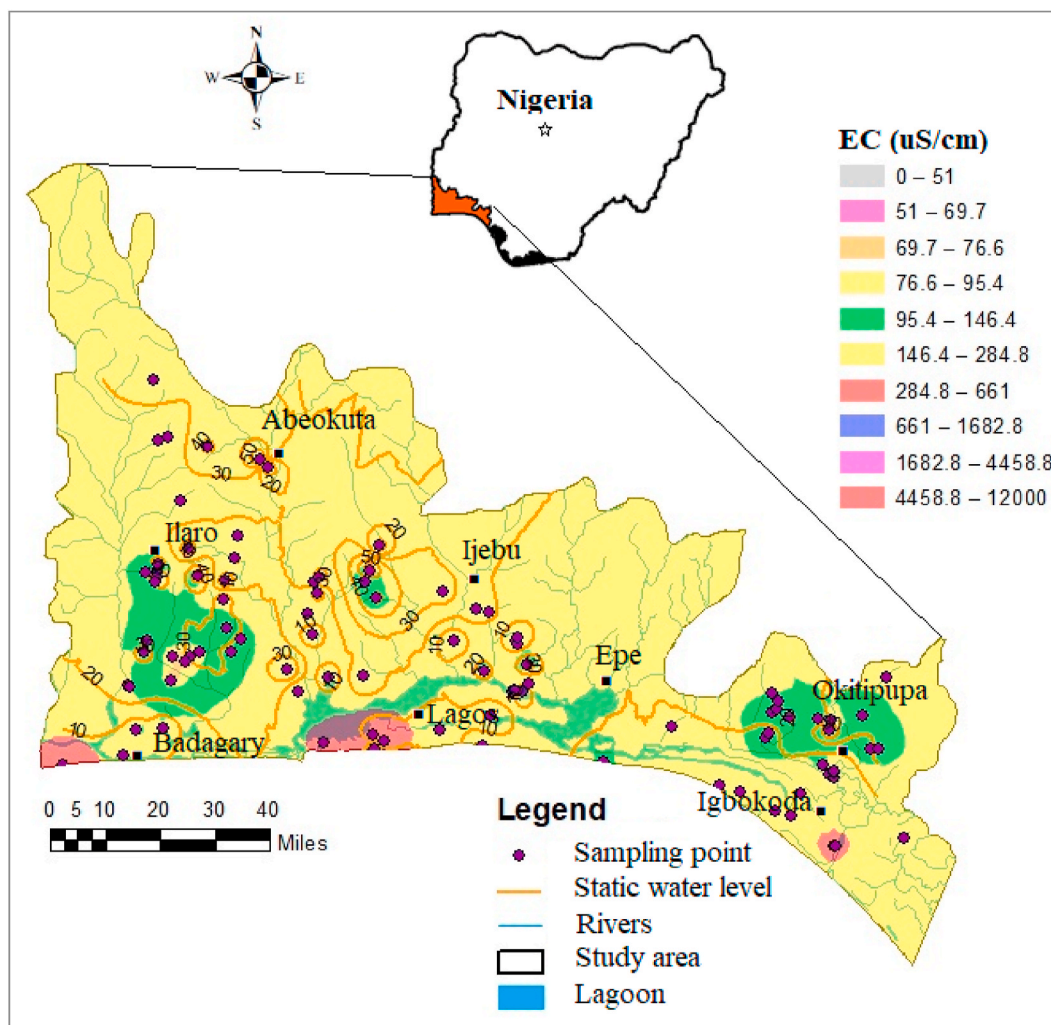


Fig. 1. Map of the Eastern Dahomey Basin showing the sampling points and spatial distribution of Electrical conductivity.

investigation is undulated at the north and flattening in to plane towards the ocean with several points virtually at or below the sea level. The highest elevation is observed around Abeokuta. Eastern Dahomey Basin is characterised by two distinct seasons, wet and dry. The wet season occurs between April and October with a break in August and features average rainfall which ranges from 1800 mm–2500 mm, while the dry season lasts from November to April (Ukhurebor and Abiodun, 2018).

The major rivers Ogun, Ose and Oluwa drain the basin into the delta and to the Atlantic Ocean. The basin hosts two major administrative water basins authorities in Nigeria, and the Ogun-Osun and Benin-Owena river basins and accommodates about 40% population of the country residence including the metropolitan city of Lagos. The study area is vital to the economy of Nigeria and West-Africa.

### 1.2. Geology and hydrogeology of Eastern Dahomey Basin

The lithological character of the sediments is formed by a regime of transgressions and regressions of the sea since the Cretaceous era, these transgressions come from the south. The stratigraphic description of the sediments has been provided by various authors including Jones and Hockey (1964); Adegoke and Omatsola (1981), Elueze and Nton (2004); Odukoya et al. (2013) Oteri and Atolagbe (2003); Ako et al. (1980); Billman (1976); Kennedy (2012); Fayose (1970); Jones and Hockey (1964), summarised in Table 1 and presented in Fig. 2. The Oligocene to Recent Alluvium Deposits and coastal plain sands consist of soft, very poorly sorted clayey sands, pebbly sands, sandy clays and rare thin lignite (Reyment, 1965). This is underlain by Ilaro formation, which consists of massive, yellowish, poorly consolidated, cross-bedded sandstones, which are fine-medium-grained and poorly sorted (Kogbe (1976). This layer is followed by Ewekoro formation which consists of predominantly paleocene fossiliferous limestone that becomes arenaceous towards the base (Reyment, 1965) and below the Abeokuta formation consists of lower Cretaceous sandstone and grits with interbedded mudstone unconformity overlaying the basement complex fine detrital sandstone, siltstone and shale.

The Coastal Plains Sands represents the main aquifer in the southern parts of the EDB, in which most of the wells and boreholes extract water. This is a multi-aquifer system consisting of three aquifer horizons separated by silty or clayey layers (Longe et al., 1987) The aquifer shows high thickness at the northern part of Abeokuta, through Ewekoro, Ilaro, and thin-out at the coast. The percentage composition of sands in lithology also increases towards the coast (Longe et al., 1987).

Longe et al. (1987) characterised coastal plain and alluvium deposits into different units. The first is an unconfined water table aquifer prone to pollution. The second and third are confined aquifers composed of an alternating sequence of sand and clay. They are tapped by boreholes as the basis of mini water-works in Lagos area. These aquifers belong to the continental Ilaro Formation. The third aquifer appears to be the most productive facies with a high level of groundwater exploitation as most

**Table 1**  
Stratigraphic Sequence in the Eastern Dahomey Basin (Modified from Adelana et al., 2004).

Formation	Age	Rock Type	Approximate Depth of Base (m.b.s.l)
Coastal Plain Sands	Tertiary (Oligocene – Pleistocene)	Clays, Silty Clays, Sands	130
Ilaro	Tertiary Eocene	Clays and Shales	280
Ewekoro	Tertiary Paleocene	Shales, limestone and sands	550
Abeokuta	Upper Cretaceous	Sandstone, Siltstone, Shale, Conglomerate	350–600
Basement complex rock	Paleozoic to Precambrian	Granites and Migmatite	>400

m.b.s.l represents metre below the sea level.

production terminates in this unit. This aquifer is in an under confined to semi-confined condition (Longe et al., 1987; Adelana et al., 1996; Longe, 2011). Generally, the piezometric surface ranges from 2.0 to 15.0 m below ground level (b.g.l) in the area. Also, the study area is well-drained by rivers and streams that flow into the lagoon and the Atlantic Ocean. The average annual precipitation is above 1700 mm and serves as a primary source of groundwater recharge.

## 2. Materials and method

### 2.1. Field physicochemical measurement and groundwater sampling

A topographical map of the study area was gridded to determine accessible locations within the area in which to carry out a systematic and representative groundwater sampling. Physicochemical measurements of Electrical conductivity (EC), pH, Total Dissolved Solids (TDS) Salinity, Redox potential (Eh) and temperature were measured and recorded in the field using Model 99,720 microprocessor pH/Conductivity meter. A total of 229 water samples were collected from shallow boreholes and hand-dug wells, 96 in the dry season and 133 in the wet season, across the Eastern Dahomey Basin. The samples were collected in three separate polyethylene bottles labelled A, B and IS Samples labelled A were acidified to a pH < 2 after collection with 0.4 ml of concentrated nitric acid (HNO<sub>3</sub>). Samples B and IS were filtered with a 0.45 µm filter and preserved in an ice-packed cooler to keep samples temperature below 4 °C before being transported to the laboratory for further analysis.

### 2.2. Laboratory analysis

Cations and anions analyses were carried out using inductively coupled plasma - optical emission spectrometry (ICP-OES) and Ion Chromatography (IC) with standard methods after filtering with <0.45 µm. Alkalinity and Bicarbonate were determined using HACH digital titrator using Bromocresol Green-Methyl red and Phenolphthalein indicator using 0.16 and 1.6 M of sulphuric acid. Results were checked for error using calculated error equations recommended by Adelana et al. (1996).

### 2.3. Data quality control

Quality control was conducted on hydrochemical laboratory results of the ions using ionic balance using (sum of cations versus the sum of anions). About 75% of the samples fall within ±5 acceptable error limit as described in Adelana et al. (1996) with 12 (dry season) and 19 (wet season) samples recorded above this threshold. Total dissolved solids (TDS) and calculated total dissolved ions (TDI) were plotted on a scatter diagram and showed a correlation of 0.78 and 0.86 respectively for both wet and dry seasons. The values are both below the limits recommended for hydrochemical analysis by the World Meteorological Organization (WMO) in 1994.

### 2.4. Data evaluation and analysis

#### 2.4.1. Theoretical background

##### 1. HFE-Diagram approach

The Hydrochemical Facies Evolution Diagram (HFE-D) proposed by Gimenez Forcada (2010) provides a simple way to identify the state of a coastal aquifer with respect to intrusion/freshening phases, as identified by the distribution of anion and cation percentages as presented in Fig. 4. The HFE-D uses only the percentage of the major cations (Ca<sup>2+</sup> and Na<sup>+</sup>) and anions (HCO<sub>3</sub><sup>-</sup>, SO<sub>4</sub><sup>2-</sup> and Cl<sup>-</sup>) to determine the dynamics of saline/saltwater intrusion. The authors suggest conventional diagrams such as the Piper diagram do not allow for full recognition of the

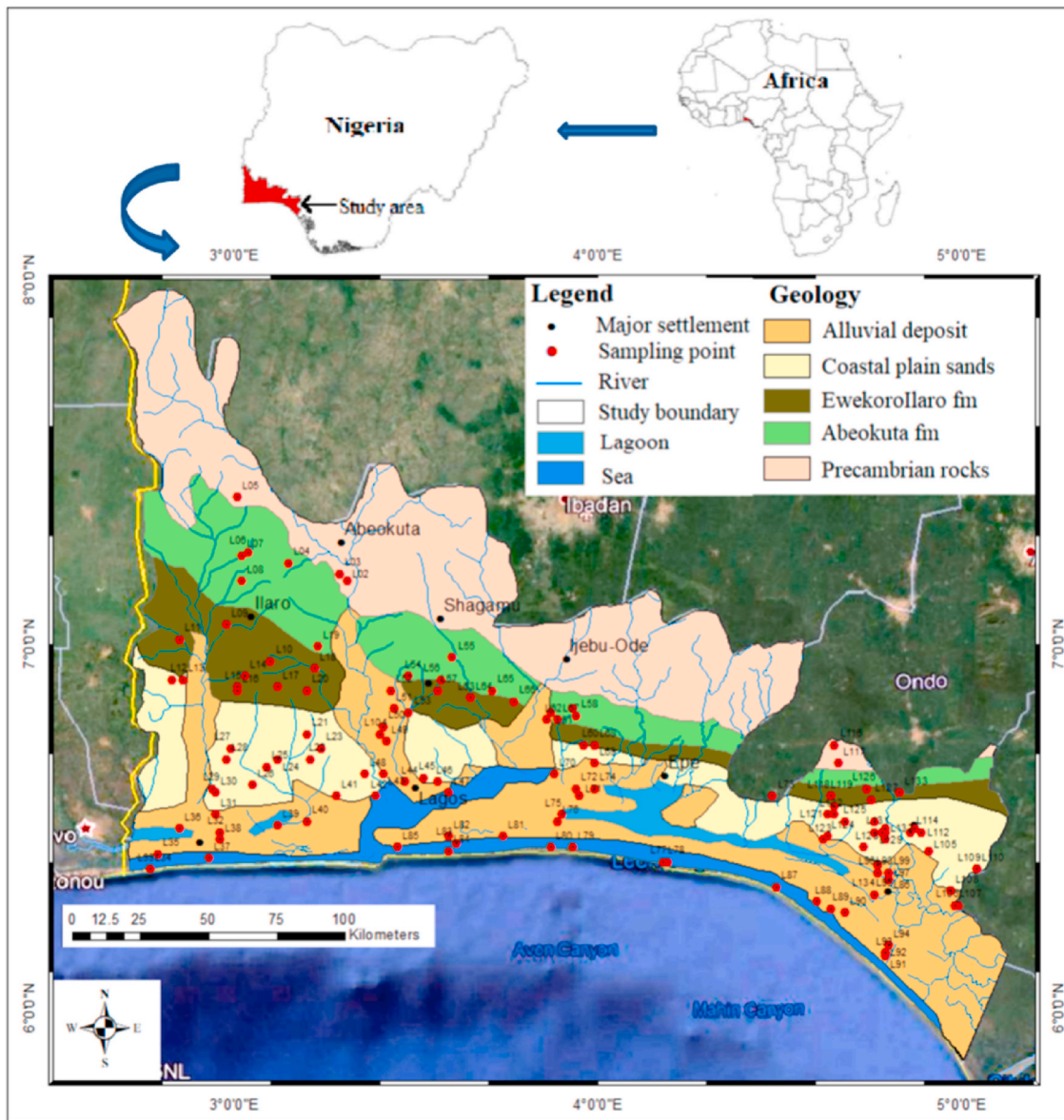


Fig. 2. Geology map of Eastern Dahomey Basin showing river drainage and Lagoon.

facies evolution sequence during recharge and intrusion events. Therefore, Gimenez Forcada (2010) suggested that the HFE-D diagram is more informative for this purpose. This diagram is well explained in Amiri et al. (2016).

2. Groundwater Quality Index for Saltwater Intrusion (GQIswi)

This method accounts for hydrochemical processes associated with saltwater intrusion and is explained using graphical methods like the Piper diagram and Chaddah or Hydrochemical facies evolution diagram. As these graphical methods are not georeferenced for use by policymakers, the approach of GQIswi is used to simplify multiple non-linear processes involving several water quality pollutants into an indicator that can be quantified and spatially referenced into a single map, (Tomaszkiewicz et al., 2014). Singhal and Gupta (2010); Edet (2016) and Amiri et al. (2016) all successfully applied this method in their studies. GQIswi is numerically derived as shown in equations below;

$$GQI_{cation} = [(1 - \%(Na+K) \times 50)] \text{ if } \%Ca < 50 \text{ or } [(1 - \%(Mg) \times 50)] \text{ if } \%Ca \geq 50 \tag{1}$$

$$GQI_{anion} = [(1 + \%(CO_3 + HCO_3) \times 25)] \text{ if } \%Cl < 50 \text{ or } [(\% (SO_4^{2+}) \times 50)] \text{ if } \%Cl \geq 50 \tag{2}$$

$$GQI_{ec} = \left[ \frac{20,000 - EC_{loc}}{20,000 - 200} \right] \text{ if } 200 \leq EC_{loc} \leq 20,000 \text{ or } 0 \text{ if } EC_{loc} \geq 20,000 \tag{3}$$

$$GQI_{swi} = \frac{GQI_{cation} + GQI_{anion} + GQI_{ec}}{2} \tag{4}$$

3. Seawater mixing index (SMI)

The ‘‘Saltwater Mixing Index’’ (SMI) proposed by Park and Aral (2008) is based on the work of Aniekan Edet (2016) and used to estimate the relative degree of saltwater/brackish water mixing with freshwater. SMI value can be computed as follows:

$$SMI = a \times \frac{C_{Na}}{T_{Na}} + b \times \frac{C_{Mg}}{T_{Mg}} + c \times \frac{C_{Cl}}{T_{Cl}} + d \times \frac{C_{SO4}}{T_{SO4}} \tag{5}$$

where letters a, b, c and d represent the relative degree concentration proportion of ions such as Na, Mg, Cl, and SO<sub>4</sub> in seawater respectively where (a = 0.31, b = 0.04, c = 0.57, d = 0.08); C is the measured concentration (in mg/l) of the ions in groundwater. The letter T represents the regional threshold values estimated from the interpretation of the probability curves as shown by Edet (2016). From the regional results in this study, the computed threshold values for Na, Mg, Cl, and SO<sub>4</sub> were 107, 18.4, 218 and 37.9 mg/l, respectively. SMI for each sample is computed using the calculated threshold values. If the SMI is greater than 1, the water is said to be affected by seawater mixing (Edet, 2016).

### 3.1. Data processing and statistical analysis

Geochemist workbench student edition 12.0 and GW-Chart by the USGS were used to plot data and determination of water type from the hydrochemical results. Descriptive statistics and Pearson's correlation coefficient between the physicochemical parameters were carried out using SPSS and Microsoft Origin Pro. The correlation coefficient (R-value) ranges between -1 and +1 provide an insight into the relationship between the pairs of the physicochemical parameters. Pearson's correlation coefficient value lies between +1 to -1, and the degree of correlation is said to be a perfect correlation if the correlation coefficient value is near +1. For values ranging between +0.75 and +1, is considered a high degree of correlation, similarly a moderate degree of correlation for values between +0.25 and +0.75 and a low degree of correlation for values between 0 and +0.25, and vice versa for the negative correlation values (Kumar et al., 2011). A correlation matrix was carried out on the data set from the two seasons separately.

#### 3.1.1. GIS approach

Results of the calculated numerical indices and water types were plotted on the map of the study area using ArcGIS version 10.60 after converting the imported CSV files to shapefiles and then plotted on a study area map extracted from a global administrative boundary map downloaded from the DIVA-GIS website. The maps present the georeferenced spatial distribution of the electrical conductivities, water type and groundwater quality index for saltwater intrusion GQIswi.

## 4. Results and discussions

### 4.1. Groundwater chemical analysis

The physical and chemical characteristics of groundwater samples from the shallow boreholes and hand-dug wells during wet (June to July 2017) and dry (February to March 2018) seasons within Eastern Dahomey Basin (EDB) coastal aquifer in Nigeria are presented in Table 2 and Fig. 3. Total dissolved solids (TDS) varies from below detection (BD) in rainwater to 8500 of the seawater from the Gulf of Guinea coast with an average of 201.8 mg/l in the wet season. In the dry season samples,

TDS ranges from 2.3 to 9300 mg/l with an average of 233 mg/l. The increase in TDS during the dry season samples could be attributed to the effect of evaporation which encourages increase in mineral concentrations in groundwater compared to the dilution process driven by precipitation in the wet season. Similarly, electrical conductivity (EC) (see Table 2) of the groundwater is higher in the dry season compared to the wet season. Major ions in groundwater, such as Cl, Na, SO<sub>4</sub> and Mg<sup>2+</sup>, are used as an indication of saltwater intrusion into freshwater aquifer and are presented in Table 2. The concentration of Cl ranges from 0.1 to 18,970 mg/l with an average value of 218 mg/l in wet season samples while those from the dry season range from 0.9 mg/l to 19,230 mg/l with an average value of 32 mg/l. Chloride concentration shows a slight increase in concentration during the dry season. The concentration of Na ranges from 0.1 to 8857 mg/l and 0.6 to 9420 mg/l with an average of 107 and 104 mg/l for wet and dry seasons, respectively. The correlation coefficient between chloride and sodium (Tables 3a and 3b) in the wet season (r = 0.01) compared to dry season (r = 0.98) indicate the diverse source of chloride, which could be attributed to anthropogenic contribution possibly effluent from sewage or leachates (Longe and Balogun, 2010; E. a Ayolabi et al., 2013; Lapworth et al., 2017). We cannot discount the impact of precipitation and evaporation, which causes mineral precipitation from the seawater and halite which characterised the dry season; however, the concentrations of sodium and chloride are far below equilibrium halite saturation.

SO<sub>4</sub><sup>2-</sup> concentration ranges from 0.1 to 2211 mg/l with an average of 245 mg/l in the wet season and 0.3–576 mg/l and the average concentration of 17.6 mg/l in groundwater samples collected during the dry season. Mg<sup>2+</sup> concentration ranges from 0.04 to 1377 mg/l with an average value of 18.4 mg/l in the wet season and 0.1–1416 mg/l with an average concentration of 18.6 mg/l in the dry season. High correlation of SO<sub>4</sub> with Cl (r = 1.0) and conversely low correlation (r = 0.05) with Na and the relatively high correlation between Cl and NO<sub>3</sub> (r = 0.60) further affirm the anthropogenic influence (see Tables 3a and 3b). Most of the increases observed in Cl, Na, Mg and SO<sub>4</sub> occurred in locations within the proximity of the sea. Cl also shows higher correlation with all the major ions except NO<sub>3</sub> in water samples from dry season. This could be attributed to the effect of salinisation resulted from saltwater intrusion and evaporation/dissolution with dominant Na-Cl and Ca-Cl water type (see Tables 4a and 4b).

### 4.2. Groundwater characterisation using HEF diagram

The Hydrochemical Facies Evolution Diagram (HFE-D) developed by Giménez-Forcada et al. (2010) was employed in this study. The method has been used by several authors namely Charette and Allen (2006); Wu et al. (2010); Li et al. (2015); Amiri et al. (2016); Han et al. (2016) and Shi et al. (2018) and provides a simple way to identify the state of the coastal aquifer with respect to intrusion/freshening phases. The processes are identified by the distribution of anions and cations

**Table 2**

Statistical summary of the physicochemical properties of the groundwater samples for both seasons.

Parameter	Wet Season N = 95				Dry Season N = 133			
	Min	Max	Aver	Stdev	Min	Max	Aver	Stdev
EC (µS/cm)	13.0	12,000	295.4	1219	5.5	10,009	385	1138
TDS	8.0	8500	201.8	864	2.3	6750	233	671
Ca (mg/l)	0.4	374	16.5	41.2	0.24	428	21	53.9
Mg (mg/l)	0.1	1377	18.4	140	0.14	1417	18.6	127
Na (mg/l)	0.6	8857	106.8	903	0.6	9420	104	829
K (mg/l)	0.1	447.1	10.5	46.2	0.1	488	9.1	42.9
HCO <sub>3</sub> (mg/l)	2.0	563.6	59.7	93.6	0	8390	138	765
Cl (mg/l)	0.9	18970.2	218.1	1934	1.0	1289	32	116
SO <sub>4</sub> (mg/l)	0.1	2211.	37.9	245	0.3	576	17.6	56.3
NO <sub>3</sub> (mg/l)	0.02	259	31.8	54	0.3	312	30.5	54.6
F (mg/l)	0	1.10	0.1	0.15	0.01	1.5	0.1	0.2
Br (mg/l)	0	54.7	1.0	6.3	0.01	22	0.3	1.9

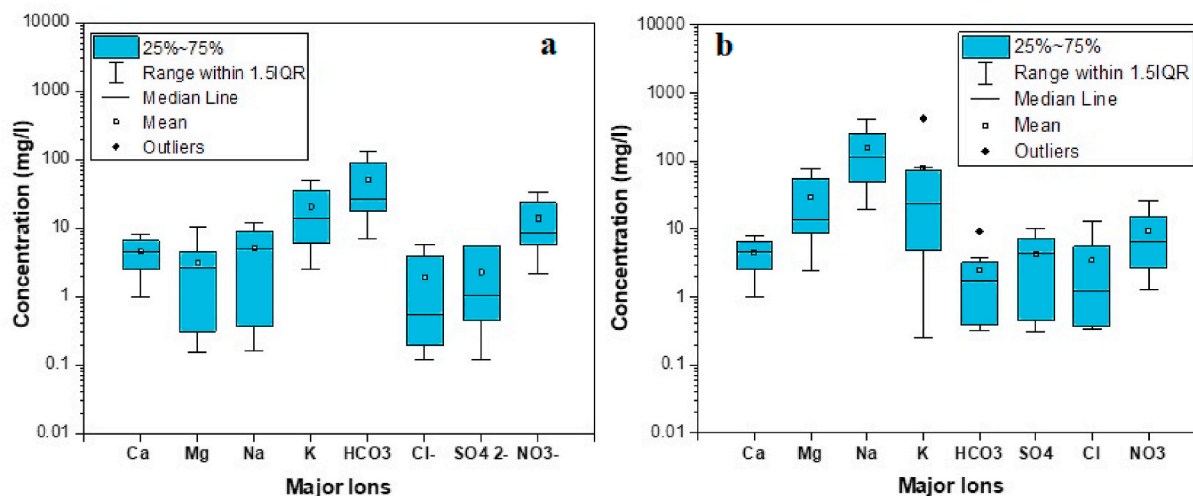


Fig. 3. Box plot for the major ions(a) Wet Season (b) dry season.

percentages in the square diagram (Fig. 5). In the HFE-Diagram, four main facies are recognised which include Na–Cl, sea/saltwater, Ca–HCO<sub>3</sub>, natural freshwater, Ca–Cl, salinised water with reverse cation exchange, and Na–HCO<sub>3</sub>, salinised water with direct cation exchange (Fig. 5). The facies explained two, almost simultaneous, processes which occur during the intrusion stage of saltwater into freshwater.

The facies types located above and to the left of the conservative mixing line are representative of the freshening phase whereas facies types situated below and to the right of the line characterise the sea/saltwater intrusion phase. Facies types located in the centre of HFE-diagram can be considered as a mixing phase for both fresh and saltwater representing the transformation phase for either freshening or intrusion phases. In the intrusion and freshening fields, various sub-steps can be identified, following the salinity evolution through the Cl<sup>−</sup> percentage. The freshening sub-steps include f-1, f-2, f-3, f-4, and FW (representative of freshwater composition). In this diagram, the intrusion sub-steps related to the sea/saltwater intrusion phase are represented as i-1, i-2, i-3, i-4, and SW (representative sea/saltwater composition).

During the recharge of the aquifer, the groundwater is said to be in the freshening phase with f4 with dominant Ca–HCO<sub>3</sub> in the inland towards the northern parts of the basin bounded by the Precambrian rock which is unconformably overlain by the oldest Abeokuta formation groundwater aquifer. This facies is gradually transforming to mixed Ca + Na–HCO<sub>3</sub> rock. This begins from an initial state because the aquifer contains kaolinite which releases more Na<sup>+</sup> ions into the groundwater to form a mixed water of facies f-3 (MixNa–MixHCO<sub>3</sub>, Ca– MixHCO<sub>3</sub> and Mix). As the water continues to flow within the basin, the groundwater gradually transforms to f-2 (MixNa–MixCl) probably due to the influence of sea spraying and possible effluents from the industries as the industrial activities increase towards the same trend as groundwater flow down south. Finally, the f-1 facies represents water type which has experienced influence of saltwater intrusion and is mostly close to the coastline (see Fig. 4a, b). Na–Cl water type dominates the coastal plain sands and alluvium deposits aquifer and some locations along river channels and lagoon, especially in the rainy season. A summary of water types is shown in Tables 4a and 4b while Fig. 4a and b shows their spatial distribution across EDB for both wet and dry season, respectively. Finally, the intrusion process (salinisation) of the aquifer is reduced as the freshening increases northward towards the inland of the basin.

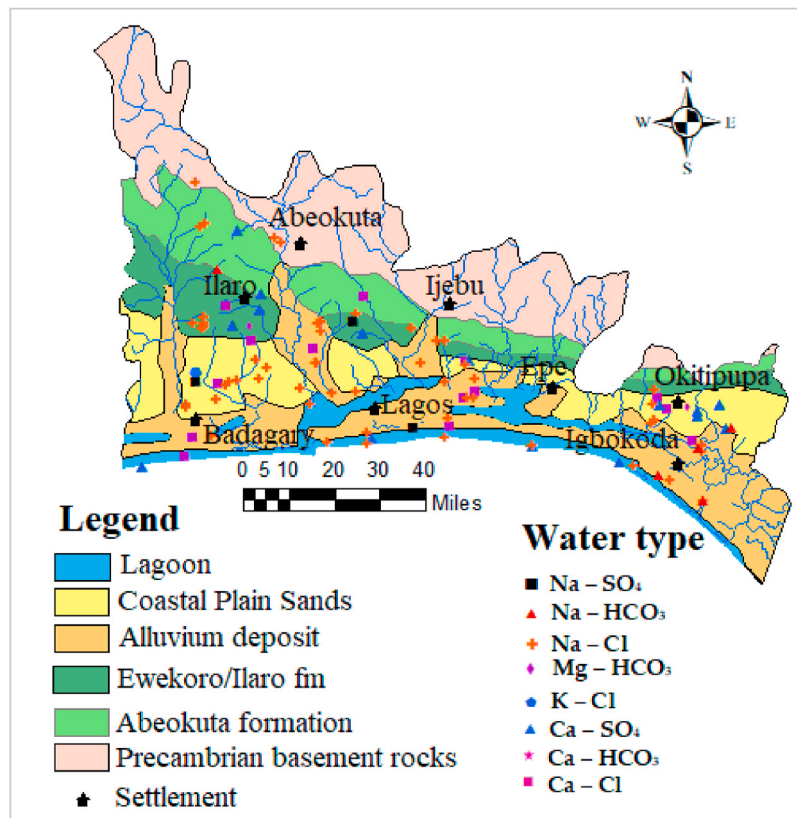
#### 4.3. Ionic ratio

Ionic ratios have been used to evaluate seawater intrusion in coastal

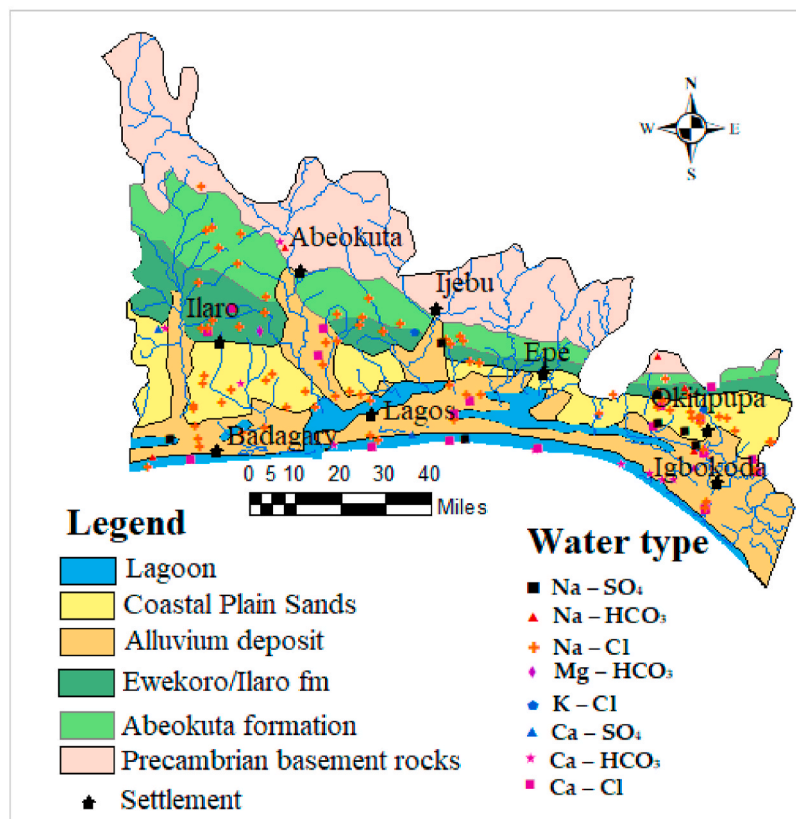
areas at different locations around the world (Custodio, 2005; Khaska et al., 2012; Li et al., 2015; Katz et al., 2010; Aniekan Edet, 2016). The ionic ratio of water samples for both wet and dry season in the basin are presented in Table 5. Tables 6a and 6b contain the correlation between EC, saltwater mixing index (SMI) and these ratios. These ratios are considered to be a good indicator of seawater intrusion. They include Na<sup>+</sup>/Ca<sup>2+</sup>, Ca<sup>2+</sup>/Cl<sup>−</sup>, Na<sup>+</sup>/Ca<sup>2+</sup>, Cl/HCO<sub>3</sub>, Mg/Cl, Ca/SO<sub>4</sub>, SO<sub>4</sub>/Cl and Cl/Br. The ratio Mg<sup>2+</sup>/Cl<sup>−</sup> shows moderate positive correlation ( $r = 0.946$ ) with Na/Cl in the wet season and ( $r = 0.919$ ) in the dry season. This correlation indicates seawater mixed in groundwater for both seasons. The Cl/Br in groundwater ranges from 4.46 to 346 (wet) and 6.45 to 460 (dry) with an average of 170 and 49 respectively. There is a weak correlation between EC and Cl/Br (Tables 6a and 6b) with ( $r = 0.192$  and  $0.297$ ) for the wet and dry seasons respectively. Higher correlation values between EC and Cl/Br in water samples during the dry season indicates more influence of seawater in the dry as compared to the wet season. This is confirmed by EC and SMI correlation which is 0.516 in the wet season and 0.931 in the dry season. This process suggests chloride in the groundwater in the wet season is more from non-seawater sources (e.g. effluent), while the groundwater in the dry season has more influence of seawater. The ratios of Na<sup>+</sup>/Cl<sup>−</sup> showed significant correlation with EC ( $r = 0.73$ ) (see Tables 6a and 6b) in the wet season and very weak ( $r = 0.070$ ) in the dry season which also confirmed the earlier statement.

##### 4.3.1. Revelle coefficient, [Cl/(CO<sub>3</sub>+HCO<sub>3</sub>)] ratio

The Revelle Coefficient (Cl/(CO<sub>3</sub>+HCO<sub>3</sub>)) ratio has been used as a criterion to evaluate the saltwater intrusion in previous groundwater studies (Abdalla, 2016; Edet, 2016; Kumar et al., 2010). Chloride is one of the dominant ions in seawater and mostly occurs in small amounts in groundwater. HCO<sub>3</sub> is usually the most abundant negative ion in groundwater while it occurs in low concentration in seawater. The ration of these anions is used as a measure of the degree of contamination of freshwater by saltwater. The classification is shown in Table 7. In this study, 55.2 and 45.9% of the sampled groundwater fell into the category of good quality water with respect to Cl/HCO<sub>3</sub> ratio for wet and dry seasons respectively, while 39.6 and 42.9% of the samples showed slight seawater influence for the respective season. Seawater influence was observed on 2.25% of the samples from the dry season and 0% from the wet season. The highest seawater impact is observed in water samples from wells located around Okun-Ajjah, Ode-Mahin and Gbetomey. These are less than 500 m from the coastline except Ode-Mahin which is within 100 m from the sea lagoon. Only one sample collected showed extreme influence expected from seawater. This result



a. Distribution of groundwater types for the water samples during the wet season



b. Distribution of groundwater types in the dry season

Fig. 4. a. Distribution of groundwater types for the water samples during the wet season. b. Distribution of groundwater types in the dry season.

**Table 3a**  
Pearson correlation for the physicochemical parameters for wet season samples.

Param	EC	TDS	Ca	Mg	Na	K	HCO3	Cl-	SO4	NO3-	F	Br
EC	1											
TDS	1.00	1.00										
Ca	0.94	0.94	1.00									
Mg	0.99	0.99	0.91	1.00								
Na	0.99	0.99	0.90	1.00	1.00							
K	0.98	0.98	0.93	0.98	0.98	1.00						
HCO <sub>3</sub>	0.15	0.14	0.46	0.09	0.05	0.14	1.00					
Cl-	0.06	0.05	0.14	0.00	0.01	0.12	0.26	1.00				
SO <sub>4</sub> <sup>2-</sup>	0.10	0.10	0.18	0.04	0.05	0.16	0.28	1.00	1.00			
NO <sub>3</sub> <sup>-</sup>	0.32	0.32	0.33	0.26	0.27	0.38	0.19	0.60	0.48	1.00		
F	0.05	0.04	0.22	0.01	-0.02	0.08	0.63	0.50	0.50	0.16	1.00	
Br	0.52	0.51	0.55	0.47	0.48	0.57	0.25	0.88	0.90	0.29	0.43	1

2-Tailed Test of Significance.

**Table 3b**  
Pearson correlation for the physicochemical parameters for dry season samples.

Para	EC	TDS	Ca	Mg	Na	K	HCO <sub>3</sub>	Cl	SO <sub>4</sub>	NO <sub>3</sub>	F	Br
EC	1											
TDS	1.00	1.00										
Ca	0.90	0.90	1.00									
Mg	0.97	0.97	0.82	1.00								
Na	0.99	0.99	0.76	0.99	1.00							
K	0.44	0.44	0.72	0.96	0.98	1.00						
HCO <sub>3</sub>	0.86	0.87	0.85	0.99	0.98	0.94	1.00					
Cl	0.95	0.95	0.65	0.88	0.98	0.45	0.33	1.00				
SO <sub>4</sub>	0.43	0.43	0.75	0.60	0.28	0.31	0.85	0.30	1.00			
NO <sub>3</sub>	0.27	0.28	0.27	0.12	0.27	0.63	0.20	0.25	0.16	1.00		
F	0.30	0.30	0.42	0.37	0.23	0.13	0.49	0.18	0.25	0.15	1.00	
Br	0.88	0.88	0.50	0.84	0.94	0.30	0.19	0.96	0.16	0.05	0.13	1.00

2-Tailed Test of Significance.

**Table 4a**  
Groundwater type with water their respective sample locations for dry season.

Water Type	Sample	% Sample	Sample Location
Na-Cl	56	58.3	L02, L04, L05, L07, L08, L09, L12, L13, L14, L15, L16, L22, L23, L24, L25, L26, L28, L29, L32, L33, L36, L38, L39, L41, L42, L43, L45, L46, L47, L48, L49, L49, L50, L52, L53, L55, L56, L57, L58, L60, L62, L63, L65, L67, L69, L71, L72, L74, L76, L77, L80, L81, L82, L85, L87, L88 and L89
Na-SO <sub>4</sub>	3	3.1	L31, L51 and L68
Na-HCO <sub>3</sub>	5	7.3	L10, L75, L78, L79 and L96
Ca-HCO <sub>3</sub>	15	15.6	L03, L06, L17, L18, L19, L35, L54, L66, L70, L73, L84, L92, L93, L94 and L95
Ca-Cl	14	14.6	L01, L11, L21, L27, L34, L37, L40, L44, L59, L61, L64, L83, L86 and L90
K-Cl	1	1	L30
Mg-HCO <sub>3</sub>	2	2.1	L20 and L91

further confirms the applicability of this method in the evaluation of groundwater quality with regard to saltwater intrusion (Narany et al., 2014). Comparing the results of the wet season with the dry season, there is a slightly higher intrusion in the dry season which could be attributed to over-abstraction of groundwater when common rain harvesting stopped while dilution could be responsible for low salinity in the wet season (Table 7).

Chloride concentration was classified into fresh, fresh-brackish, brackish, brackish-salt, salt and hyperhaline as shown in Table 8. The results revealed 97.92% and 95.5% water fall within the freshwater class for wet and dry seasons respectively. This method only shows the slight effect of seasonal variation on saltwater intrusion with 1.0% and 0.7% which represent the only sample collected from the sea as the saltwater among the samples while 2.3% of the dry season groundwater samples

**Table 4b**  
Groundwater type with water their respective sample locations for dry season.

Water Type	Sample	% Sample	Sample Location
Na-Cl	81	60.9	L01, L04, L05, L06, L07, L08, L09, L11, L14, L15, L17, L18, L19, L22, L23, L25, L26, L27, L28, L29, L30, L31, L32, L33, L34, L38, L39, L40, L41, L42, L43, L44, L45, L46, L47, L48, L49, L51, L53, L54, L55, L56, L57, L58, L59, L60, L61, L63, L64, L65, L67, L68, L69, L70, L72, L73, L74, L76, L82, L83, L94, L96, L99, L101, L104, L105, L107, L110, L112, L114, L115, L117, L118, L120, L121, L125, L127, L129, L130, L131 and L132
Na-SO <sub>4</sub>	7	5.3	L36, L62, L79, L100, L119, L124 and L128
Na-HCO <sub>3</sub>	6	4.5	L02, L35, L111, L116, L126 and L134
Ca-HCO <sub>3</sub>	12	9	L03, L13, L24, L78, L85, L86, L87, L88, L89, L90, L95 and L98
Ca-Cl	21	15.8	L10, L102, L106, L108, L109, L122, L123, L133, L16, L37, L50, L52, L71, L75, L77, L80, L84, L91, L92, L93 and L97
Ca-SO <sub>4</sub>	3	2.3	L12, L81 and L113
K-Cl	2	1.5	L66 and L103
Mg-HCO <sub>3</sub>	1	0.8	L20

indicate brackish-salt water compared to 0% of the wet season.

4.4. Assessment of intrusion using saltwater mixing index (SMI)

The seawater mixing index (SMI) which was proposed by Par et al. (2005) was also employed in this study to further assess the groundwater of the Eastern Dahomey Basin with respect to seawater pollution. The results of this method are presented in Table 9. The results show that 96.9 and 93.2 per cent of the groundwater samples from both wet and dry seasons fall within a freshwater category with SMI values below 1.0,

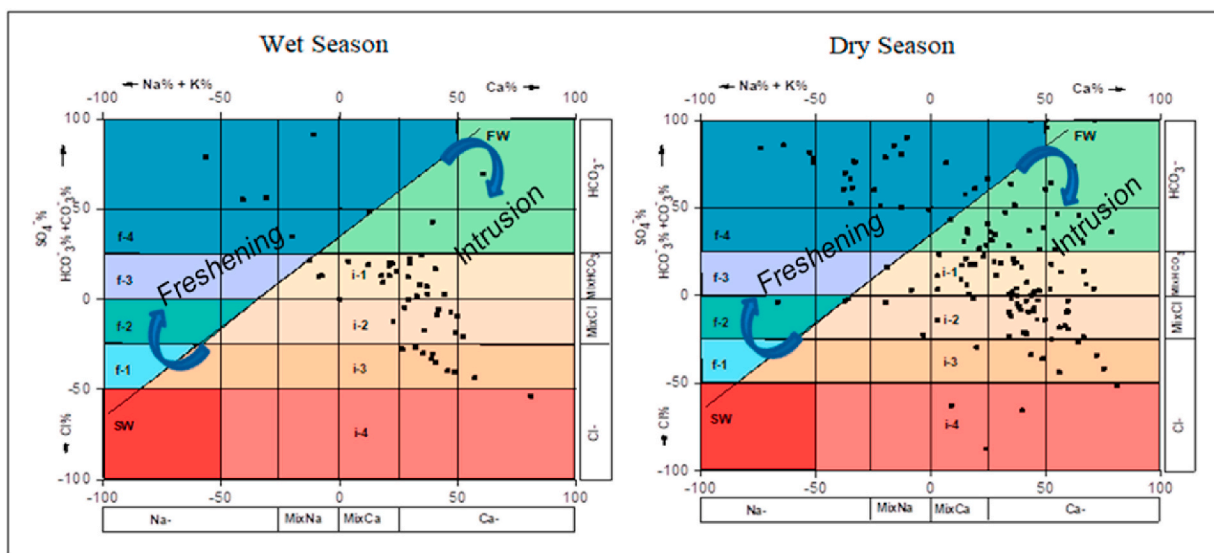


Fig. 5. Hydrochemical plots for major ions in analysed groundwater samples from Eastern Dahomey Basin aquifers. (A) HEF diagram which indicates mixing of saline water in a few locations within the coastal plain sand aquifers.

Table 5  
Statistic Summary of TDS, SMI and some selected Ionic ratio.

Ionic Ratio	Wet Season N = 96				Dry Season N = 133			
	Min	Max	Aver	Stdev	Min	Max	Aver	Stdev
HCO <sub>3</sub> /Cl	0.01	39.09	4.23	6.63	0.063	77.583	6.777	16.026
Na/Cl	0.01	67.83	1.55	6.88	0.02	53.128	3.764	10.913
Na/Ca	0.09	23.68	2.27	3.01	0.574	7.22	2.709	1.51
Ca/Cl	0.00	11.43	1.04	1.73	0.01	14.804	1.406	3.126
K/Cl	0.00	3.42	0.32	0.49	0.006	19.18	1.504	3.98
Cl/HCO <sub>3</sub>	0.03	67.42	1.25	6.84	0.013	15.962	1.364	3.252
Mg/Cl	0.00	10.55	0.34	1.13	0.006	6.484	0.497	1.327
Ca/SO <sub>4</sub>	0	0	0	0	0.035	33.41	4.641	8.729
SO <sub>4</sub> /Cl	0.00	5.88	0.53	0.87	0.041	3.171	0.598	0.833
Cl/Br	4.46	346.96	170.96	53.08	6.449	460.343	49.178	100.277
SMI	0.00	54.68	0.99	6.29	0.009	0.306	0.056	0.077

Table 6a  
Correlations between the ionic ratios for wet season water sample.

	EC	Ca/Cl	Na/Cl	Na/Ca	Cl/HCO <sub>3</sub>	Mg/Cl	Ca/SO <sub>4</sub>	SO <sub>4</sub> /Cl	Cl/Br	SMI
EC	1.000									
Ca/Cl	0.123	1.000								
Na/Cl	0.985	0.148	1.000							
Na/Ca	0.707	-0.157	0.735	1.000						
Cl/HCO <sub>3</sub>	0.042	-0.092	-0.033	0.008	1.000					
Mg/Cl	0.934	0.299	0.946	0.632	-0.046	1.000				
Ca/SO <sub>4</sub>	-0.018	-0.016	-0.029	-0.008	-0.033	-0.021	1.000			
SO <sub>4</sub> /Cl	0.043	0.303	0.074	-0.027	-0.083	0.091	-0.208	1.000		
Cl/Br	0.192	-0.017	0.128	0.013	-0.004	0.099	0.282	-0.038	1.000	
SMI	0.516	-0.004	0.450	0.333	0.875	0.414	-0.048	-0.038	0.077	1.000

2-Tailed Test of Significance.

while 1.1 and 2.3% of respective wet and dry season samples are slightly polluted based on SMI with values falling between 1.0 and 2.0. 2.08 and 3.0% of wet and dry season water samples revealed SMI values between 10.0 and 150.0, which indicate dangerously polluted groundwater with saltwater intrusion. This represents the groundwater from Gbetomey in Badagary, Ogombo, Okun-Ajjah and Ode-Mahin in the wet and dry season. In addition to those mentioned earlier, the Isheri and Adesanya areas near Lekki during the dry season samples also revealed high SMI values. This is also supported by the moderate to high correlation value between SMI, EC and Cl/HCO<sub>3</sub> with a correlation coefficient of 0.51 and 0.88 (Table 6a) in the wet season while SMI, EC and Na/Cl revealed

correlation values of 0.93 and 0.50 but low correlation value of -0.02 with Cl/HCO<sub>3</sub> in the dry season samples (Table 6b). The variation in these correlation could be attributed to effect of sea spraying which salt dissolution in precipitation in the wet season and evaporation concentration/mineral dissolution in the dry season (Vengosh and Rosenthal, 1994; Abimbola et al., 1999; Edet, 2019).

4.5. Groundwater quality index in relation to saltwater intrusion

The aquifer monitoring and vulnerability maps for saltwater intrusion were prepared based on calculations of GQI<sub>SWI</sub> and HFE diagrams

**Table 6b**  
Correlations between the ionic ratios for dry season water sample.

Ionic ratio	EC	Ca/Cl	Na/Cl	Na/Ca	Cl/HCO3	Mg/Cl	Ca/SO4	SO4/Cl	Cl/Br	SMI
EC	1.000									
Ca/Cl	0.097	1.000								
Na/Cl	0.070	0.755	1.000							
Na/Ca	-0.007	-0.269	0.063	1.000						
Cl/HCO <sub>3</sub>	0.042	-0.165	-0.082	0.048	1.000					
Mg/Cl	0.127	0.824	0.919	-0.068	-0.123	1.000				
Ca/SO <sub>4</sub>	0.006	0.382	0.378	-0.082	-0.118	0.452	1.000			
SO <sub>4</sub> /Cl	0.078	0.179	0.009	-0.122	-0.085	0.046	-0.256	1.000		
Cl/Br	0.297	-0.061	-0.101	-0.228	0.232	-0.079	0.049	0.019	1.000	
SMI	0.931	0.061	-0.007	0.504	-0.017	0.113	-0.014	0.139	0.381	1.000

2-Tailed Test of Significance.

**Table 7**  
Groundwater Quality Classification based on Cl/HCO3 ratio.

Classification	Cl/ HCO <sub>3</sub>	Wet Season		Dry Season	
		Samples	% Sample	Sample	% Sample
Good Quality	<0.5	53	55.21	61	45.9
Slightly Contaminated	0.5-1.3	36	39.58	57	42.9
Moderately Contaminated	1.3-2.8	6	6.25	12	9.02
Highly Contaminated	2.8-6.6	0	0	3	2.25
Extremely Contaminated	>6.6	1	1.04	0	0

**Table 8**  
Classification of water, based on Chloride Content.

Water Class	Wet Season Chloride (mg/l)	Dry Season	
		Sample	%Sample
Fresh	≤150	94	97.9
Fresh-brackish	150-300	1	1.1
Brackish	300-1000	0	0
Brackish-Salt	1000-10,000	0	0
Salt	10,000-20,000	1	1.1
Hyperhaline	> 20,000	0	0

**Table 9**  
Classification of seawater mixing index (SMI).

SMI Range	Classification	Wet Season		Dry Season	
		Sample	% Sample	Sample	% Sample
<1	Freshwater	93	96.9	124	93.2
1.0-2.0	Slightly polluted	1	1.04	3	2.3
2.0-6.0	Moderately polluted	0	0	1	0.75
6.0-10.0	Seriously polluted	0	0	1	0.75
10.0-150.0	Dangerously polluted	2	2.08	4	3.01
>150	Seawater	0	0	0	0

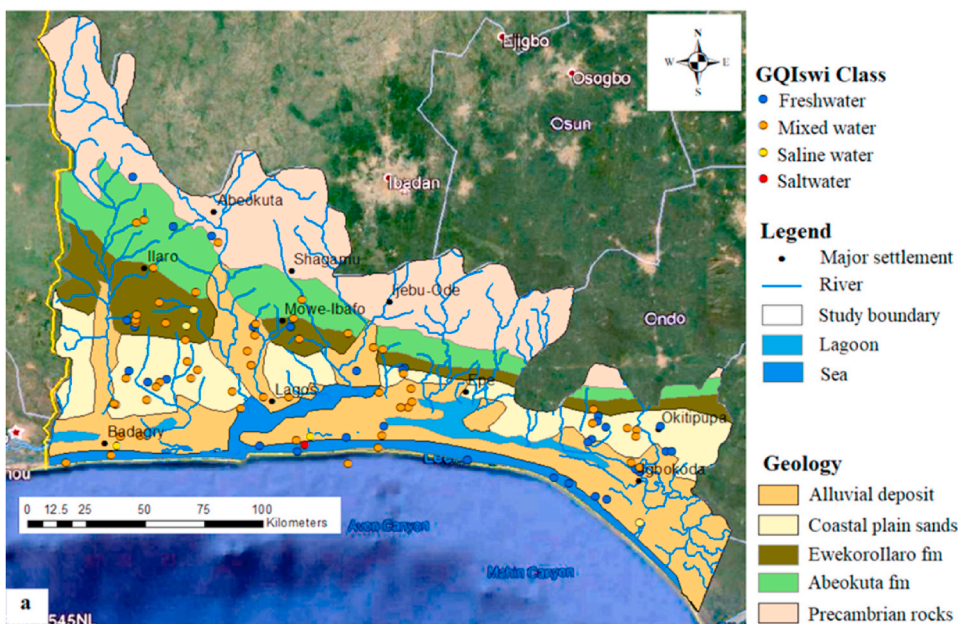
**Table 10**  
Summary of Indices evaluated for Wet and Dry season.

Index	Wet Season N = 96				Dry Season N = 133			
	Min	Max	Aver	Stdev	Min	Max	Aver	Stdev
GQI <sub>pipermix</sub>	11.84	90.84	45.88	16.87	17.12	90.3	45.55	15.49
GQI <sub>pipermixdom</sub>	22.12	84.29	45.36	6.4	18.91	87.58	51.43	12.24
F <sub>sea</sub> (%)	-0.11	99.01	1.04	10.21	-0.11	6.7	0.05	0.65
GQI <sub>fsea</sub>	-4.34	111.19	-3.85	1020.96	-1.94	111.26	95.32	64.96
GQI <sub>swi</sub>	-9.67	99.68	21.02	511.89	-10	99.27	70.43	34.46

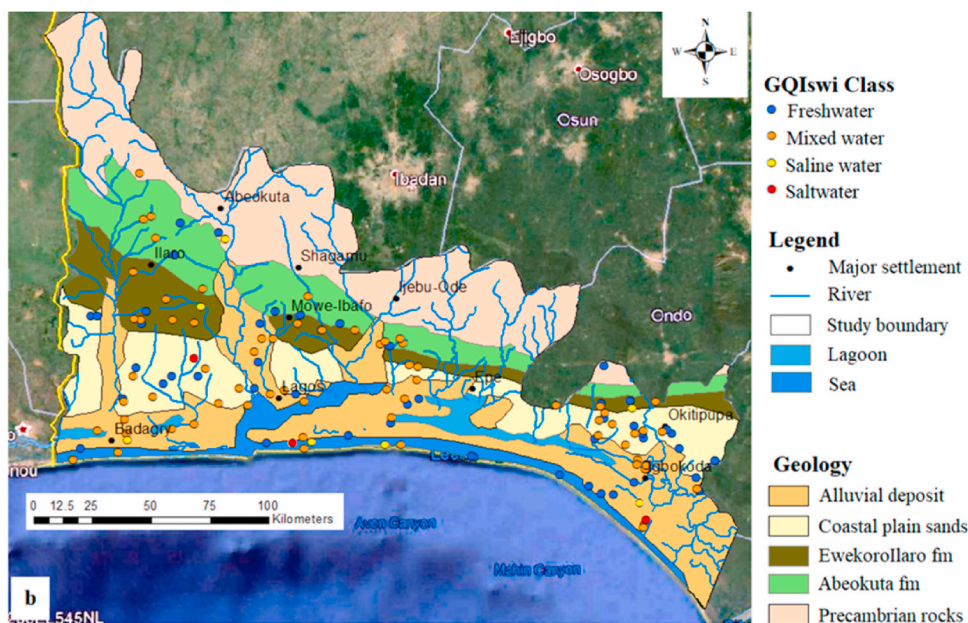
for both wet and dry seasons. Based on GQI<sub>SWI</sub> method as presented in Tables 10 and 11, the spatial distribution maps (Fig. 6) revealed that the study area is dominated by freshwater in both wet (mean GQI<sub>SWI</sub> = 21.0) and dry seasons (mean GQI<sub>SWI</sub> = 70.4). However, some fingerprint of saltwater intrusion was identified in both seasons in locations along the coastline due to their proximity to the Gulf of Guinea. Saline water was identified in some locations far inland into the basin especially along the rivers during the wet season. Low correlation of Na and Cl (r = 0.01) in wet season and a conversely high value (r = 0.98) implies a different origin of Cl in groundwater. Higher correlation of Cl with NO<sub>3</sub> (r = 0.60) in the wet season suggests anthropogenic influence which could be attributed to high recharge and soil saturation rate, while a relatively low correlation value (r = 0.25) between Cl and NO<sub>3</sub> suggests geogenic sources of seawater intrusion and evapoconcentration in the dry season. A few boreholes within 500 m of the coastline located at the south-central to the southwestern part within the coastal plain sand and alluvium deposit show relatively higher salinity. This higher salinity is suspected to be an indication of a saltwater intrusion. Processes such as over-abstraction of water from the shallow aquifer, flooding triggered by sea-level rise due to climate change and effluence from domestic and municipal waste might contribute to future increases in the salinity of groundwater within this basin (Aladejana et al., 2020). Total evaporation with precipitation of halite minerals along the riverbed has been reported in a few areas (E. a. E.A. Ayolabi et al., 2013; Odukoya et al., 2013). It is important to note that halite is not considered a major source of salinity as freshwater predominates the areas along the coastline, where most of the shallow wells tap the unconfined aquifer that is directly recharged by the precipitation. The GQI<sub>swi</sub> show mixed groundwater types as predominant groundwater across the Eastern Dahomey Basin. This predomination of mixed groundwater type based

**Table 11**  
Results of GQI<sub>swi</sub> calculated for water samples in wet and dry seasons.

Water type	Typical GQI <sub>swi</sub>		Wet Season		Dry Season	
	Min	Max	Samples	% Sample	Samples	%Sample
Freshwater	75	100	30	32	58	43.6
Mixed GW	50	75	64	68.75	67	50.4
Saline GW	10	50	1	1.04	6	4.5
Saltwater	0	10	1	1.04	2	1.5



a. Spatial variation of groundwater quality index for saltwater intrusion (GQIswi) of the Eastern Dahomey Basin during the wet season



b. Spatial variation of groundwater quality index for saltwater intrusion (GQIswi) of the Eastern Dahomey Basin during the dry season

Fig. 6. a. Spatial variation of groundwater quality index for saltwater intrusion (GQIswi) of the Eastern Dahomey Basin during the wet season. b. Spatial variation of groundwater quality index for saltwater intrusion (GQIswi) of the Eastern Dahomey Basin during the dry season.

on GQIswi is also supported by the hydrochemical facies evolution diagram (HFE-D) earlier presented in Fig. 5. The mixing characteristics observed across this Basin could be attributed to the nature (geology) of the basin through rock-water interaction and also to topography (gravity) driven flow generally in a north-south direction (Fig. 6).

5. Conclusion

In this study, saltwater intrusion into the freshwater aquifer of the Eastern Dahomey Basin, Southwestern Nigeria, was monitored using a seasonal hydrochemical quality index and ionic ratios such as HFE-D, SMI and GQIswi and Ionic ratio such as Cl/Br, Cl/HCO3 that are used

to evaluate seawater intrusion. Pearson correlation analysis physico-chemical parameters, especially  $Na^+$ ,  $Ca^{2+}$ ,  $Mg^{2+}$ ,  $Cl^-$ ,  $HCO_3^-$  and  $SO_4^{2-}$  and EC values revealed the influence of seawater intrusion in some of the water samples from wells that are relatively deeper within the proximity of the coastline of Seme, Lekki, Eleko, Okun-Ajjah, Ode-Mahin and Igbokoda. It further revealed the anthropogenic influence of industrial and municipal effluent especially in samples from wells within the alluvium deposit which are generally closer to the river channels flood plain. Results of HFE-D, Ionic ratios, SMI and GQIswi revealed that mixed groundwater of  $Na + Ca-HCO_3$  and  $Na-Cl$  dominate the area due to gravity-driven flow.

Spatial distribution of groundwater revealed freshening, which

increases inland from the coastline towards the northern part of the basin. Results of the groundwater quality index confirmed this and identified few locations of saline water around Lekki, Okun-Ajjah and the Ode-Mahin in both wet and dry seasons. Most sampled boreholes show freshwater during the wet season above the units characterised by saltwater intrusion. The present study provides important information to support planners and policy-makers to develop sustainable water resources management plans for the region to prevent deterioration of the freshwater resources of coastal groundwater in the Eastern Dahomey Basin.

### Declaration of competing interest

The authors declare that they have no known competing financial interests or personal relationships that could have appeared to influence the work reported in this paper.

### Acknowledgements

The Author is grateful to the Petroleum Technology and Development Fund (PTDF) under the Overseas PhD scholarship scheme for funding this research and also for the support of the Scottish Government under the Climate Justice Fund Water Futures Programme, awarded to the University of Strathclyde (Prof R.M. Kalin).

### Appendix A. Supplementary data

Supplementary data to this article can be found online at <https://doi.org/10.1016/j.gsd.2021.100568>.

### References

- Abdalla, F., 2016. Ionic ratios as tracers to assess seawater intrusion and to identify salinity sources in Jazan coastal aquifer, Saudi Arabia. *Arab. J. Geosci.* 9, 1–12. <https://doi.org/10.1007/s12517-015-2065-3>.
- Abimbola, A.F., Tijani, M.N., Nurudeen, A., 1999. Some aspect of groundwater quality assessment of Abeokuta. *J. Min. Geol.* 32, 23–32.
- Adegoke, O.S., Omatsola, M.E., 1981. Tectonic evolution and cretaceous stratigraphy of the Dahomey Basin. *Niger. J. Min. Geol.* 18, 130–137.
- Adelana, S.M.A., Olasehinde, P.I., Bale, R.B., Vrbka, P., Edet, A.E., Goni, I.B., 1996. An overview of the geology and hydrogeology of Nigeria. *Q. J. Eng. Geol. Hydrogeol.* 29, S1–S12. <https://doi.org/10.1144/GSL.QJEGH.1996.029.S1.01>.
- Aladejana, J.A., Kalin, R.M., Sentenac, P., Hassan, I., 2020. Assessing the impact of climate change on groundwater quality of the shallow coastal aquifer of eastern Dahomey Basin, southwestern Nigeria. *Water* 12, 224. <https://doi.org/10.3390/w12010224>.
- Amiri, V., Nakhaei, M., Lak, R., Kholghi, M., 2016. Assessment of seasonal groundwater quality and potential saltwater intrusion: a study case in Urmia coastal aquifer (NW Iran) using the groundwater quality index (GQI) and hydrochemical facies evolution diagram (HFE-D). *Stoch. Environ. Res. Risk Assess.* 30, 1473–1484. <https://doi.org/10.1007/s00477-015-1108-3>.
- Ayolabi, E. a, Folorunso, A.F., Odukoya, A.M., Adeniran, A.E., 2013. Mapping saline water intrusion into the coastal aquifer with geophysical and geochemical techniques : the University of Lagos campus case ( Nigeria ), 2. Springer plus, pp. 1–14. <https://doi.org/10.1186/2193-1801-2-433>.
- Ayolabi, E.A., Folorunso, A.F., Kayode, O.T., 2013. Integrated geophysical and geochemical methods for environmental assessment of municipal dumpsite system. *Int. J. Geosci.* 4, 850–862. <https://doi.org/10.4236/ijg.2013.45079>.
- Charette, M.A., Allen, M.C., 2006. Precision ground water sampling in coastal aquifers using a direct-push, shielded-screen well-point system. *Ground Water Monit. Remed.* 26, 87–93. <https://doi.org/10.1111/j.1745-6592.2006.00076.x>.
- Christina, G., Alexandros, G., 2014. Seawater intrusion and nitrate pollution in coastal aquifer of almyros – nea anchialos basin , Central Greece. *WSEAS Trans. Environ. Dev.* 10, 211–222.
- Custodio, E., 2005. Coastal aquifers as important natural hydrogeological structures. In: Taylor and Francis (ED) *Groundwater and Human Development*, Chapter 3, pp. 15–38, 1905–1918.
- Edet, A., 2016. Hydrogeology and groundwater evaluation of a shallow coastal aquifer, southern Akwa Ibom State (Nigeria). *Appl. Water Sci.* <https://doi.org/10.1007/s13201-016-0432-1>.
- Edet, A., 2019. Seasonal and spatio-temporal patterns, evolution and quality of groundwater in Cross River State, Nigeria: implications for groundwater management. *Sustain. Water Resour. Manag.* 5, 667–687. <https://doi.org/10.1007/s40899-018-0236-6>.
- Giménez-Forcada, E., Bencini, A., Pranzini, G., 2010. Hydrogeochemical considerations about the origin of groundwater salinization in some coastal plains of Elba Island (Tuscany, Italy). *Environ. Geochem. Health* 32, 243–257. <https://doi.org/10.1007/s10653-009-9281-2>.
- Han, D., Song, X., Currell, M.J., 2016. Identification of anthropogenic and natural inputs of sulfate into a karstic coastal groundwater system in northeast China: evidence from major ions,  $\delta^{13}\text{C}_{\text{DIC}}$  and  $\delta^{34}\text{S}_{\text{SO}_4}$ . *Hydro. Earth Syst. Sci.* 20, 1983–1999. <https://doi.org/10.5194/hess-20-1983-2016>.
- Jones, H.A., Hockey, R., 1964. The geology of part of southwestern Nigeria. *GSN Bull.* No. 31–10.
- Kennedy, G.W., 2012. Development of a Gis-Based Approach for the Assessment of Relative Seawater Intrusion Vulnerability in Nova Scotia. Canada.
- Kumar, K.S., Kumar, P.S., Babu, M.J.R., Rao, C.H., 2010. Assessment and mapping of ground water quality using geographical information systems. *Int. J. Eng. Sci. Technol.* 2, 6035–6046.
- Kumar, P.J.S., Jegathambal, P., James, E.J., 2011. Multivariate and geostatistical analysis of groundwater quality in palar river basin. *Int. J. Geol.* 5, 108–119.
- Lapworth, D.J., Nkhuwa, D.C.W., Okotto-Okotto, J., Pedley, S., Stuart, M.E., Tijani, M.N., Wright, J., 2017. Urban groundwater quality in sub-Saharan Africa: current status and implications for water security and public health. *Hydrogeol. J.* 25, 1093–1116. <https://doi.org/10.1007/s10040-016-1516-6>.
- Li, W., Wang, M.-Y., Liu, L.-Y., Yan, Y., 2015. Assessment of long-term evolution of groundwater hydrochemical characteristics using multiple approaches: a case study in cangzhou, northern China. *Water* 7, 1109–1128. <https://doi.org/10.3390/w7031109>.
- Longe, E.O., 2011. Groundwater resources potential in the coastal plain sands aquifers. *Lagos , Nigeria* 3, 1–7.
- Longe, E.O., Balogun, M.R., 2010. Groundwater quality assessment near a municipal landfill, Lagos, Nigeria. *Res. J. Appl. Sci. Eng. Technol.* 2, 39–44.
- Longe, E.O., Malomo, S., Olorunniwo, M.A., 1987. Hydrogeology of Lagos metropolis. *J. Afr. Earth Sci.* 6, 163–174. [https://doi.org/10.1016/0899-5362\(87\)90058-3](https://doi.org/10.1016/0899-5362(87)90058-3).
- Narany, T.S., Ramli, M.F., Aris, A.Z., Nor, W., Sulaiman, A., Juahir, H., Fakharian, K., 2014. Identification of the hydrogeochemical processes in groundwater using classic integrated geochemical methods and geostatistical techniques. *Amol-Babol Plain , Iran. Sci. World J.* 1–15, 2014.
- Odukoya, A.M., Folorunso, A.F., Ayolabi, E.A., Adeniran, E.A., 2013. Groundwater quality and identification of hydrogeochemical processes within university of Lagos , Nigeria. *J. Water Resour. Protect.* 5, 930–940. <https://doi.org/10.4236/jwarp.2013.510096>.
- Oteri, A.U., Atolagbe, F.P., 2003. Saltwater intrusion into coastal aquifers in Nigeria. The Second International Conference on Saltwater Intrusion and Coastal Aquifers — Monitoring, Modeling, and Management. Mérida, Yucatán, México, March 30 - April 2, 2003. Merida Yucatan, pp. 1–15.
- Park, C.H., Aral, M.M., 2008. Saltwater intrusion hydrodynamics in a tidal aquifer. *J. Hydro. Eng.* 13, 863–872. [https://doi.org/10.1061/\(ASCE\)1084-0699\(2008\)13:9\(863\)](https://doi.org/10.1061/(ASCE)1084-0699(2008)13:9(863)).
- Saha, R., Dey, N.C., Rahman, S., Galagedara, L., Bhattacharya, P., 2018. Exploring suitable sites for installing safe drinking water wells in coastal Bangladesh. *Groundw. Sustain. Dev.* 7, 91–100. <https://doi.org/10.1016/j.gsd.2018.03.002>.
- Saha, R., Dey, N.C., Rahman, M., Bhattacharya, P., Rabbani, G.H., 2019. Geogenic arsenic and microbial contamination in drinking water sources: exposure risks to the coastal population in Bangladesh. *Front. Environ. Sci.* 7, 1–12. <https://doi.org/10.3389/fenvs.2019.00057>.
- Seddique, A.A., Masuda, H., Anma, R., Bhattacharya, P., Yokoo, Y., Shimizu, Y., 2019. Hydrogeochemical and isotopic signatures for the identification of seawater intrusion in the paleobeach aquifer of Cox's Bazar city and its surrounding area, south-east Bangladesh. *Groundw. Sustain. Dev.* 9 <https://doi.org/10.1016/j.gsd.2019.100215>.
- Shi, X., Wang, Y., Jiao, J.J., Zhong, J., Wen, H., Dong, R., 2018. Assessing major factors affecting shallow groundwater geochemical evolution in a highly urbanized coastal area of Shenzhen City, China. *J. Geochem. Explor.* 184, 17–27. <https://doi.org/10.1016/j.gexplo.2017.10.003>.
- Talabi, A.O., Tijani, M.N., Aladejana, A.J., 2012. Assessment of impact of climatic change on groundwater quality around Igbokoda Coastal area , southwestern Nigeria. *J. Environ. Earth Sci.* 2, 39–50.
- Tirkey, P., Bhattacharya, T., Chakraborty, S., Baraik, S., 2017. Assessment of groundwater quality and associated health risks: a case study of Ranchi city, Jharkhand, India. *Groundw. Sustain. Dev.* <https://doi.org/10.1016/j.gsd.2017.05.002>.
- Tomaszkiewicz, M., Abou Najm, M., El-Fadel, M., 2014. Development of a groundwater quality index for seawater intrusion in coastal aquifers. *Environ. Model. Software* 57, 13–26. <https://doi.org/10.1016/j.envsoft.2014.03.010>.
- Ukhurebor, K.E., Abiodun, I.C., 2018. Variation in annual rainfall data of forty years (1978-2017) for south-south, Nigeria. *J. Appl. Sci. Environ. Manag.* 22, 511. <https://doi.org/10.4314/jasem.v22i4.13>.
- Wu, M.-L., Wang, Y.-S., Sun, C.-C., Wang, H., Dong, J.-D., Yin, J.-P., Han, S.-H., 2010. Identification of coastal water quality by statistical analysis methods in Daya Bay, South China Sea. *Mar. Pollut. Bull.* 60, 852–860. <https://doi.org/10.1016/j.marpolbul.2010.01.007>.